J. Cell. Mol. Med. Vol 13, No 11-12, 2009 pp. 4505-4521

Differential involvement of the extracellular 6-O-endosulfatases Sulf1 and Sulf2 in brain development and neuronal and behavioural plasticity

Ina Kalus [a], Benedikt Salmen [b], Christoph Viebahn [c], Kurt von Figura [d], Dietmar Schmitz [b], Rudi D´Hooge [e], Thomas Dierks [a, *]

[a] Department of Chemistry, Biochemistry I, Bielefeld University, Bielefeld, Germany
[b] Neuroscience Research Center, Charité – Universitätsmedizin Berlin, Berlin, Germany
[c] Department of Anatomy and Embryology, Centre of Anatomy, University of Göttingen, Göttingen, Germany
[d] Department of Biochemistry II, University of Göttingen, Göttingen, Germany
[e] Laboratory of Biological Psychology, Department of Psychology, University of Leuven, Leuven, Belgium

Received: June 20, 2008; Accepted: October 10, 2008

Abstract

The extracellular sulfatases Sulf1 and Sulf2 remove specific 6-O-sulfate groups from heparan sulfate, thereby modulating numerous signalling pathways underlying development and homeostasis. *In vitro* data have suggested that the two enzymes show functional redundancy. To elucidate their *in vivo* functions and to further address the question of a putative redundancy, we have generated Sulf1- and Sulf2-deficient mice. Phenotypic analysis of these animals revealed higher embryonic lethality of Sulf2 knockout mice, which can be associated with neuroanatomical malformations during embryogenesis. Sulf1 seems not to be essential for developmental or postnatal viability, as mice deficient in this sulfatase show no overt phenotype. However, neurite outgrowth deficits were observed in hippocampal and cerebellar neurons of both mutant mouse lines, suggesting that not only Sulf2 but also Sulf1 function plays a role in the developing nervous system. Behavioural analysis revealed differential deficits with regard to cage activity and spatial learning for Sulf1- and Sulf2-deficient mouse lines. In addition, Sulf1-specific deficits were shown for synaptic plasticity in the CA1 region of the hippocampus, associated with a reduced spine density. These results reveal that Sulf1 and Sulf2 fulfil non-redundant functions *in vivo* in the development and maintenance of the murine nervous system.

Keywords: heparan sulfate proteoglycans • Sulf1 • Sulf2 • synaptic plasticity • behaviour • neurite outgrowth

Introduction

Heparan sulfate proteoglycans (HSPGs) mediate interactions of cells with their environment by binding to growth factors, morphogens, cytokines, chemokines, matrix ligands and cell surface molecules. In the nervous system, where HSPG expression is dynamically regulated, they are involved in important processes such as neurite outgrowth, neuronal migration and synaptic plasticity [1–4]. These glycoconjugates are composed of heparan sulfate (HS) chains, consisting of repeating disaccharide units, attached to core proteins. The enzymes Exostosin (Ext) 1 and 2 catalyse HS polymerization [5–7]. Specific removal of Ext1 function from embryonic day 12.5 in conditional knockout mice confirmed the importance of HSPGs for the developing nervous system [8]. The resulting lack of all HS led to gross malformations in brain patterning combined with severe guidance errors.

Apart from core protein variety, the complexity of HSPGs is further based on specific HS modifications, namely epimerization, de-acetylation and sulfation. After the HS chain is polymerized by the Ext enzymes resulting in alternating N-acetylglucosamine (GlcNAc) and glucuronic acid (GlcA) residues, members of the *N*-deacetylase/*N*-sulfotransferase enzyme family (NDSTs) generate clusters of disaccharide units with *N*-sulfated glucosamine (GlcNS) residues. A C5-epimerase then can act on GlcA residues to form iduronic acid (IdoA). Thereupon 2-, 6- and infrequently also 3-O-sulfotransferases modify the nascent HS chain [5–7]. These highly dynamic enzyme activities generate specific structural codes within the HS chain. Also here the knockout of enzymes acting downstream of Ext1 revealed the importance of

*Correspondence to: Thomas DIERKS,
Department of Chemistry, Biochemistry I, Bielefeld University,
Universitätsstr. 25, 33615 Bielefeld, Germany.
Tel.: 49-521-106-2092
Fax: 49-521-106-6014
E-mail: thomas.dierks@uni-bielefeld.de

doi:10.1111/j.1582-4934.2008.00558.x

© 2008 The Authors
Journal compilation © 2009 Foundation for Cellular and Molecular Medicine/Blackwell Publishing Ltd

HS sulfation patterns and epimerization. Lack of the NDST-1 results in a severe cerebral and craniofascial phenotype [9]. Furthermore, embryos lacking heparan sulfate-6-O-sulfotransferase-1 or heparan sulfate-2-O-sulfotransferase show aberrant axon navigation specific for each sulfotransferase [10].

So far only two enzymes are known which are able to modify existing HS codes after the newly synthesized proteoglycan has left the secretory pathway, namely the extracellular 6-O-endosulfatases Sulf1 and Sulf2 [11, 12]. The genetic knockout or gene-trap disruption of these sulfatases has been described recently [13–17]. Sulf1 and Sulf2 cleave 6-O-sulfate moieties from HS chains, thereby influencing the activity of growth factors like Wnt, fibroblast growth factor-2 (FGF-2), stromal cell-derived factor-1 (SDF-1), bone morphogenetic proteins (BMPs), glial derived neurotrophic factor (GDNF) and hepatocyte growth factor (HGF) [15, 18–24]. While numerous *in vitro* studies have analysed growth factor signalling pathways influenced by the action of Sulf1 and Sulf2, little is known about their *in vivo* function, in particular in the nervous system.

In this study, we investigated the significance of Sulf functionality for the murine brain, where the two enzymes are highly and differentially expressed during development and adulthood (for summary, see Table 1). We show that Sulf deficiency affects brain development, neurite outgrowth of cerebellar and hippocampal neurons, synaptic plasticity, as well as learning and motor activity. Sulf1 and Sulf2 deficiency differentially contribute to these impairments.

Materials and methods

Mouse lines

Sulf1 and Sulf2 knockout mouse lines were generated as described previously [13]. In brief, gene targeting vectors were electroporated into 129 ola embryonic stem cells. A positive ES clone, genotyped for a single and specific recombination event using Southern blotting with 5' and 3' external as well as internal probes, was injected into C57BL/6 blastocysts to produce chimeric mice. Male chimeras were mated with C57BL/6 females, which led to germ-line transmission of the targeted alleles. From these, heterozygotes were intercrossed to generate wild-type and knockout littermates (hybrid C57BL/6 $\times$ 129 ola background). Furthermore chimeras with germ-line transmission were bred with 129 ola females and heterozygous littermates were intercrossed to generate Sulf1- and Sulf2-deficient lines with 129 ola background. In general, for all experiments presented in this study, knockout and wild-type littermates with hybrid C57Bl/6 $\times$ 129 ola background were used with the exception of the lightmicroscopical analysis of hydrocephalic Sulf2-deficient mice for which additionally Sulf2-deficient hydrocephalic mice of the 129 ola line were analysed. The mice were bred, housed and handled according to the local animal ethics committee (AZ. 604.45502/01–24.95).

Light microscopical analysis

Wild-type and hydrocephalic Sulf2-deficient mice from postnatal to adult stages, were fixed for at least 7 days with Bouin's fixative using perfusion (7 days old to adult) or immersion fixation (early postnatal stages) and decalcified using 5–7% nitric acid for 3 (young stages) to 7 (adult) days prior to embedding in paraffin wax, serial sectioning in the transverse plane at 10 μm and staining of sections using haematoxylin and eosin.

Nissl staining

Fixed vibratome sections (5 μm) were incubated with 0.5% cresyl violet in acetate buffer for 15 min. at room temperature, dehydrated in ascending series of aqueous ethanol (70%, 90% and 100%), followed by xylol and mounted with Roti-Histokit (Carl-Roth, Karlsruhe, Germany).

Immunofluorescence microscopy

Cryosections (5 μm) were fixed for 15 min. at room temperature with PBS containing 4% formalin. After three washing steps with PBS and blocking of unspecific binding by incubation with PBS containing 5% FCS and 0.05% Triton X-100 for 1 hr at room temperature, slices were incubated with mouse monoclonal antibodies against Neurofilament L (1:30, Cell Signaling Technology, Danvers, MA, USA) and rabbit polyclonal antibodies against GFAP (1:100, Cell Signaling Technology) dissolved in PBS containing 0.05% Triton X-100 for 2 hrs at room temperature followed by three washing steps with PBS. After incubation with secondary antibodies antimouse Alexa Fluor-488 (1:400, Invitrogen, Karlsruhe, Germany) and antirabbit Alexa Fluor-546 (1:400, Invitrogen) for 1 hr at room temperature and three further washing steps slices were mounted with Mowiol (Sigma-Aldrich, Taufkirchen, Germany). Before mounting, slices were counterstained with DAPI.

Timm's staining

Timm's staining was performed to visualize mossy fibres in the inner molecular layer of the hippocampus. Cryosectioned material (20 μm) was stained through a non-perfusion protocol: Therefore sections were incubated in a desiccation chamber overnight containing Na_2S solution (0.1%) that had been adjusted to pH 7.3 with 1 N HCl to form H_2S gas. The following day slices were rehydrated (95%, 70%, 50% aqueous EtOH and distilled water) and stained with Timm's staining solution (2.5% citric acid, 2.4% sodium citrate, 1.7% hydrochinone, 5% silver nitrate and 25% gum arabicum, all chemicals from Sigma-Aldrich) for 3 hrs at 30°C. Afterwards, sections were washed in tap water for 10 min. and with distilled water for 1 min. Before dehydration and mounting sections with Roti-Histokit (Carl-Roth) the reaction was stopped and background was reduced by incubating slices with 5% sodium thiosulfate solution followed by a washing step with distilled water.

Cerebella microexplant cultures

Microexplant cultures from mouse cerebella were prepared as previously described in detail [25]. Briefly, cerebella taken from 6-day-old Sulf1- or Sulf2-deficient mice and wild-type controls (see below) were forced through a Nitrex net with a pore size of 300 μm. Thirty to forty tissue pieces were plated onto poly-L-lysine (Sigma-Aldrich) coated glass coverslips (15 mm in diameter) or coverslips additionally coated with 1 μg/ml laminin (Sigma-Aldrich) and incubated in cell culture medium [MEM

© 2008 The Authors
Journal compilation © 2009 Foundation for Cellular and Molecular Medicine/Blackwell Publishing Ltd

Table 1 Sulf1 and Sulf2 mRNA expression in the developing and adult nervous system

	Sulf1 expression	***Sulf2 expression***
Embryonic stages (E9–E15, E17.5, E19.5, E21.5)		
[16, 17, 29, 30]		
Neural tube		
Floor plate	+	+
Roof plate	–	+
Forebrain		
Telencephalic vesicle	+	+
Hippocampus	–	+
Cortex	+	+
Diencephalic vesicle		
Thalamus	+	+
Hypothalamus	+	+
Eye	+	+
Midbrain	+	+
Hindbrain	+	+
Olfactory epithelium	+	–
Choroid plexus	+	+
Adult stage		
[16, 29, 30] and 'The Allen Brain Atlas Project'		
Cortex		
Lamina I	–	+
Lamina II	–	+
Lamina III	–	+
Lamina IV	–	+
Lamina V	+	+
Lamina VI	–	+
Hippocampus		
CA1	–	+
CA2	–	+
CA3	–	+
Dentate gyrus	–	+
Cerebellum		
Molecular layer	–	+
Purkinje layer	+	+
Granular layer	–	+
Choroid plexus	+	+

For detailed analysis, see Refs [17, 29, 30] and 'The Allen Brain Atlas Project' (http://www.brain-map.org).
+ expression detectable; – expression not detectable.

© 2008 The Authors
Journal compilation © 2009 Foundation for Cellular and Molecular Medicine/Blackwell Publishing Ltd

medium (PAA Laboratories, Cölbe, Germany) containing 10% horse serum (PAA Laboratories), 10% foetal calf serum (Lonza GmbH, Wuppertal, Germany), 6 mM glucose, 200 μM L-glutamine (Invitrogen), 50 U/ml penicillin (Invitrogen), 50 μg/ml streptomycin (Invitrogen), 10 μg/ml human transferrin (Sigma-Aldrich), 10 μg/ml insulin (Sigma-Aldrich) and 10 ng/ml sodium selenite (Sigma-Aldrich)]. After 16 hrs, serum-free culture medium was added to the explants and after an incubation time of further 24 hrs the explants were fixed and stained with toluidine blue/metyhlenblue. Neurite outgrowth was quantitated by measuring the length of the 10 longest neurites of fifteen aggregates in each experiment with a Leica IM1000 Image Manager (Leica, Wetzlar, Germany).

For determining the neurite length of Sulf1- and Sulf2-deficient cerebellar neurons wild-type and knockout littermates from heterozygous breedings were used. Due to tissue limitations for the statistical analysis of the neurite length of cerebellar and hippocampal neurons, cultures were prepared using newborns from homozygous knockout breedings of Sulf1- or Sulf2-deficient mice and F1 hybrid newborns from C57Bl/6 and 129 ola intercrossings as controls. The neurite length analysis of cerebellar cultures established from newborns of heterozygous intercrossing or homozygous breedings of the three described independent mouse lines revealed the same results (data not shown).

Hippocampal single cell culture

Hippocampal single cell cultures were prepared according to a published protocol [26]. Briefly, hippocampi of both hemispheres from 1-day-old Sulf1- or Sulf2-deficient mice and F1 hybrid newborns from C57Bl/6 and 129 ola intercrossings as wild-type controls were dissected in neurobasal medium (Invitrogen) containing 0.02% bovine serum albumin (BSA) and digested with 0.1% papain dissolved in neurobasal medium containing 0.02% BSA for 20 min. After digestion hippocampi were resuspended in a 1:1 mixture of cell culture medium [neurobasal medium containing 200 μM L-glutamine, 50 U/ml penicillin, 50 μg/ml streptomycin and B27-supplement (Invitrogen)] and neurobasal medium containing 1% trypsin inhibitor (Sigma-Aldrich) and 1% BSA. The tissue pieces were triturated gently through a fire polished Pasteur pipette with decreasing opening diameter. After a centrifugation step for 10 min. at 200 *g* and 4°C cells were resuspended in cell culture medium and 1×10^6 cells were plated onto poly-L-lysine coated glass coverslips (15 mm in diameter) or coverslips additionally coated with 1 μg/ml laminin. Neurite outgrowth was quantitated by measuring the length of one hundred neurites in three independent experiments with a Leica IM1000 Image Manager. For RNA preparation (see below) 1×10^7 cells were plated onto cell culture dishes (10 cm in diameter) coated with a combination of poly-L-lysine and laminin.

Cerebellar granule cells

Briefly, cerebella from 6-day-old Sulf1- or Sulf2-deficient mice and F1 hybrid newborns from C57Bl/6 and 129 ola intercrossings as wild-type controls were dissected, washed with HBSS (PAA Laboratories, Cölbe, Germany) and digested with HBSS containing 1% Trypsin (Sigma-Aldrich), 0.1% DNase (Sigma-Aldrich) and 0.8 mM $MgCl_2$ dissolved in HBSS for 20 min. After digestion cerebelli were washed twice with HBSS, resuspended in HBSS containing 0.5% DNase and were triturated through a fire polished Pasteur pipette with reducing diameter. After a centrifugation step for 10 min. and 200 *g* at 4°C cells were resuspended in cell culture medium [MEM medium (PAA Laboratories) containing 6 mM glucose, 200 μM L-glutamine (Invitrogen), 50 U/ml penicillin (Invitrogen), 50 μg/ml streptomycin (Invitrogen), 0.1% BSA, 10 μg/ml human transferrin (Sigma-Aldrich), 10 μg/ml insulin (Sigma-Aldrich), 4 nM L-thyroxine (Sigma-Aldrich), 0.027 TIU/ml aprotinin (Sigma-Aldrich) and 10 ng/ml sodium selenite (Sigma-Aldrich)]. For RNA preparation (see below) 1×10^7 cells were plated onto cell culture dishes (10 cm in diameter) coated with a combination of poly-L-lysine and laminin.

Mouse embryonic fibroblast cultures

Mouse embryonic fibroblasts were prepared as described previously [13]. For RNA preparation 1×10^7 cells were plated onto cell culture dishes (15 cm in diameter) and maintained for 48 hrs at 37°C before RNA preparation.

RNA preparation

Total RNA was isolated from wild-type, Sulf1- and Sulf2-deficient mouse embryonic fibroblasts, hippocampal and cerebellar single cell cultures using Trizol reagent according to manufacturer's protocol under RNase free conditions (Invitrogen). Due to tissue limitations the used primary neuronal cultures were established from Sulf1- or Sulf2-deficient or F1 hybrid newborns from C57Bl/6 and 129 ola intercrossings as wild-type controls. Afterwards, the samples were DNase I treated in order to remove genomic DNA contamination and the RNA quality was determined using the Agilent 2100 Bioanalyzer (Agilent Technologies, Böblingen, Germany) microfluidic electrophoresis. Only sample pairs with comparable RNA integrity numbers (typically >7.5) were selected.

cDNA synthesis

After RNA preparation and DNase I digestion cDNA synthesis from 1 μg total mRNA of wild-type, Sulf1- and Sulf2-deficient mouse embryonic fibroblasts, cerebellar granule cells and hippocampal neurons was performed using the Transcriptor First Strand cDNA Synthesis Kit (Roche Applied Science, Mannheim, Germany) according to the manufacturer's protocol.

Real-time PCR

Real-time PCR was performed using a Light Cycler 2.0 System (Roche Applied Science) and reaction mixtures were set up according to manufacturer's instructions using the Light Cycler Fast Start DNA Master Plus SYBR Green I Kit (Roche Applied Science); briefly, for a 20 μl reaction, 2 μl Primer Mix (10 pmol/μl per Primer (Forward/Reverse)), 4 μl Master Mix, 9 μl dH_2O and 5 μl cDNA template. The following primer sets from IBA GmbH (Göttingen, Germany) were designed using the Primer 3 Input 0.4.0 software, to amplify gene-specific sequences: for Sulf1 F: 5′-CTGTGTCT-GCTTGGTTGGTAGT-′3 and R: 5′-CCCGCAGGATTTATTTCTTACC-′3, for Sulf2 F: 5′-CATGACCGCTCACACGTAACC-3′ and R: 5′-ACACAGGACACA-CATCAACTTG-3′. The expression of RPL was used for standardization of cDNAs (F: 5′-ATTGTGGCCAAGCAGGTA-3′ and R: 5′-CTGGCCTCTCTTG-GTCTTGT-3). Each primer/cDNA set was used in triplicates. Data analysis was performed using the Δ Ct method normalizing against the housekeeping gene RPL. Primer efficiencies were determined with 10-fold dilution series.

© 2008 The Authors
Journal compilation © 2009 Foundation for Cellular and Molecular Medicine/Blackwell Publishing Ltd

Electron microscopy

Three-month-old Sulf1- or Sulf2-deficient mice and their wild-type controls were anaesthetized using pentobarbital and perfused intracardially with 0.9% saline, followed by 1.5% glutaraldehyde and 1.5% paraformaldehyde in phosphate buffer. Whole brains were dissected carefully, *i.e.* without touching the cerebral surface, and postfixed for 1–2 hrs in the same fixative. To investigate hippocampal regions which can be directly compared between different individual animals two consecutive coronal slices, each 1 mm thick, were taken immediately rostral to the cerebellar-cerebral junction using razor blades under stereomicroscopical control; slices were fixed overnight in the same fixative followed by 2-hr fixation in 1% osmium tetroxide in phosphate buffer. After dehydration and embedding in Araldite® using standard procedures, semithin (1 μm thick) and ultrathin sections (70–80 nm thick) were cut in alternating sequences from the CA1 region of the coronal slice surface facing the other coronal slice from the same animal. Ultrathin sections were mounted on single-slit copper grids, counterstained with lead citrate and uranyl acetate and photographed in a Zeiss electron microscope (EM9) connected to a digital camera (Mega View III, Soft Imaging Systems, Münster, Germany) at magnifications from 7000× to 55,000×. Counts of asymmetrical postsynaptic densities (PSDs) were performed on 30 neighbouring photographs taken from the stratum radiatum at the 7000 magnification (each photograph thus representing a tissue area of 9 × 13.5 um), one set of 30 photographs being taken in three different parallel planes each, each plane being separated by ten 1-micron-thick sections, in each animal. Statistical analysis on synapse density was performed by taking the average density in each animal, *i.e.* the average being calculated from the 90 counting frames in each animal and compared across genotypes using Student's t-test.

Electrophysiological recordings

Sulf1- and Sulf2-deficient mice (1 and 3 months old, as indicated in figure legend) and their wild-type controls were used in all electrophysiological experiments. Animals were anaesthetized, decapitated and the brains removed as described previously [27]. Horizontal hippocampal slices were cut at 400 μm thickness in an ice-cold solution containing 87 mM NaCl, 75 mM sucrose, 26 mM $NaHCO_3$, 2.5 mM KCl, 1.25 mM NaH_2PO_4, 0.5 mM $CaCl_2$, 7 mM $MgCl_2$, 25 mM glucose, and saturated with 95% O_2/5% CO_2. All recordings were done at room temperature in a physiological solution containing 119 mM NaCl, 26 mM $NaHCO_3$, 2.5 mM KCl, 1 mM NaH_2PO_4, 2 mM $CaCl_2$, 1.3 mM $MgCl_2$, 10 mM glucose and equilibrated with 95% O_2 and 5% CO_2. Recordings of focal field EPSP (fEPSP) were performed in the stratum radiatum with glass pipettes filled with artificial CSF (ACSF) and the pipette tip broken under visual control. Basal synaptic transmission was monitored at 0.05 Hz. The inter-theta burst stimulation (TBS) interval was 20 sec., and four TBSs were applied to induce LTP. TBS consisted of 10 bursts delivered at 5 Hz. Each burst consisted of four pulses delivered at 100 Hz. Duration of pulses was 0.2 ms, and stimulation strength was set to provide fEPSPs with an amplitude of ~50% from the subthreshold maximum. Recordings were made in the stratum radiatum. Signals were amplified 1000× and filtered at 1 KHz. Data were stored and analysed using IgorPro4.1 software (Wavemetrics, Portland, OR, USA).

Cage activity and neuromotor testing

Three-month-old Sulf1- and Sulf2-deficient mice, and wild-type littermates of Sulf2-deficient intercrossings as controls, were used in all behavioural experiments. For cage activity recording, mice were put individually in 20 × 30 cm^2 transparent cages placed between 3 IR photo beams connected to a lab-built activity logger. Activity (expressed as beam crossings) was measured for 24 hrs. Motor coordination and equilibrium were tested on an accelerating rotarod (MED Associates Inc., St. Albans, VT, USA). Mice were first trained at constant speed (4 rpm, 2 min.) before starting with four test trials (intertrial interval, 10 min.). During these test trials, the animals balanced on a rotating rod that accelerated from 4 to 40 rpm in 5 min. Time until they dropped from the rod was recorded up to 5-min. cut-off. Grip strength was measured using a device consisting of a T-shaped bar connected to a digital dynamometer (Ugo Basile, Comerio, Italy). Mice were placed before the bar, which they usually grabbed spontaneously, and gently pulled backwards until they released the bar (10 readouts were recorded per animal).

Exploratory activity

Open field exploration was examined using a 50 × 50 cm^2 square arena. Animals were dark adapted for 30 min., and placed in the arena for 10 min. each. Mice started from a specific corner of the arena, and recording of the explorative pattern began after 1 min. of adaptation. Movements in the arena were recorded using video tracking and software (Noldus, Wageningen, The Netherlands). Perambulation was recorded in different virtual areas of the arena, including a centre area, 4 corner areas (10 × 10 cm^2 squares) and a peripheral area (10 cm wide strip along the wall). Social exploration was assessed in the same arena, but 2 mice were now placed in a centrally located cage that allowed visual, olfactory and limited physical contact. Mice started from a specific corner of the arena, and recording of the explorative pattern began after 1 min. of adaptation. Total path lengths, path length in the virtual annulus around the cage, and number of approaches were recorded for 10 min. as measures of social exploration. Finally, the elevated plus maze was used to assess anxiety-related exploration. The arena consisted of a plus-shaped maze with two arms (5 cm wide) closed by side walls, and two arms without walls. Mice were placed at the centre of the maze, and were allowed to explore freely for 10 min. Exploratory activity was recorded by 5 IR beams (4 for arm entries, and 1 for open arm dwell) connected to a computerized activity logger.

Passive avoidance and spatial learning

Passive avoidance learning was assessed using a 2-compartment box that consisted of an illuminated and a dark compartment, separated by a guillotine door. After 30-min. dark adaptation, the mouse was placed in the light part and latency to enter the dark compartment was recorded. Upon entry into the dark compartment, the door was closed and a brief foot shock (1 s, 0.2 mA) was applied. The mouse was then removed from the box and placed in its home cage. Twenty-four hours later, latency to enter the dark compartment was measured in the same way.

Spatial memory abilities were examined in the hidden-platform version of the Morris maze. A 150-cm circular pool was filled with water (kept at 26°C), opacified with non-toxic white paint. A 15-cm round perspex platform was hidden at a fixed position, 1 cm beneath the surface of the water. Daily trial blocks consisted of 4 swimming trials (intertrial interval, 15 min.) starting randomly from each of 4 starting positions. Mice that failed to find the platform within 2 min. were guided to the platform, where they remained for 15 sec. before being returned to their cages. Probe trials were conducted after 5 and 10 acquisition trial blocks. During these

© 2008 The Authors
Journal compilation © 2009 Foundation for Cellular and Molecular Medicine/Blackwell Publishing Ltd

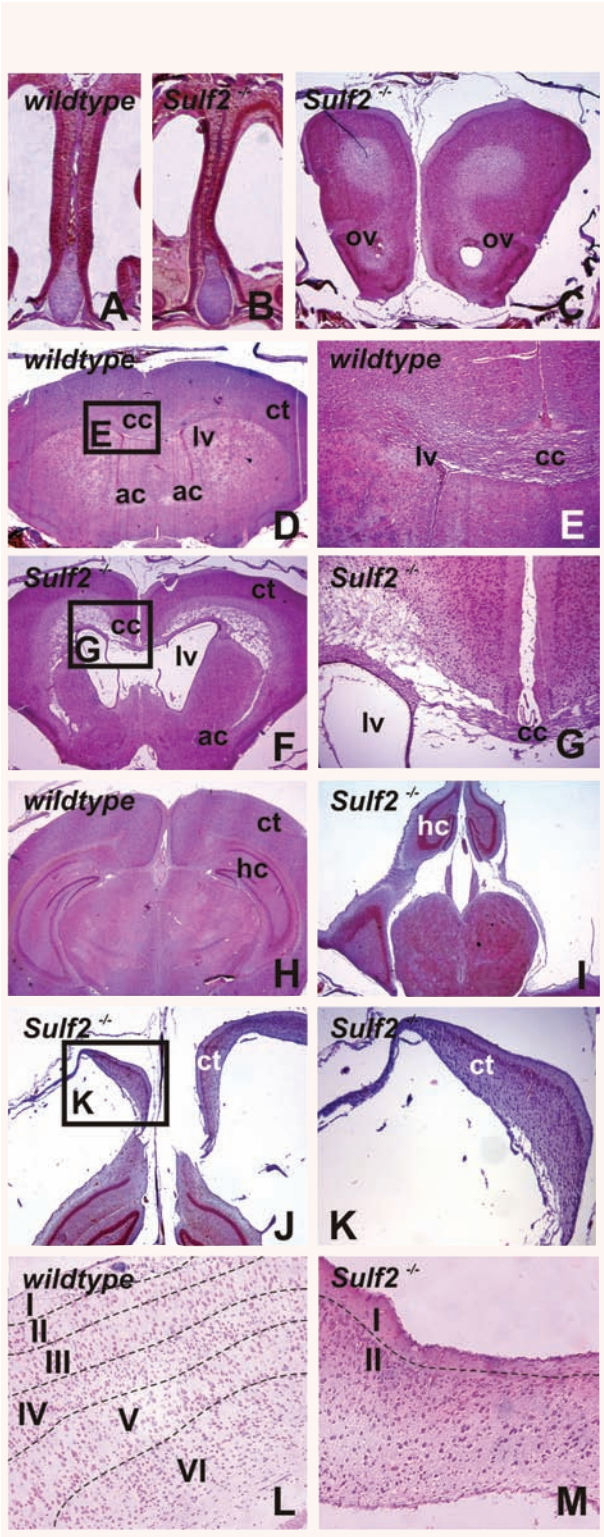

probe trials, the platform was removed from the pool, and the search pattern of the mice was recorded for 100 s. Swimming paths of the animals were recorded during all trials using video tracking and software (Noldus, Wageningen, The Netherlands).

Results

A significant fraction of Sulf2-deficient newborn mice develop a hydrocephalus

To analyse the *in vivo* function of the HS modulating enzymes Sulf1 and Sulf2, knockout mice were generated using a classical knockout approach [13]. Although both sulfatases are ubiquitously expressed in the embryo and are involved in many important signalling pathways like Wnt, FGF-2, SDF-1, BMPs, GDNF and HGF [15, 18–23], Sulf1-deficient mice show no apparent phenotype. In contrast, Sulf2 knockout mice show a small but significant reduction in litter size and body weight [14]. This rather inconspicuous phenotype of Sulf2-deficient mice at first sight agrees with the results of the phenotypic analysis of Sulf2 gene trap mice which have no major developmental defects and are viable and fertile [16, 17]. In the classical knockout situation, however, we observed Sulf2-deficient newborns displaying a hydrocephalus at birth, referred to as *congenital hydrocephalus*, which resulted in a life span shorter than 2 weeks. The percentage of hydrocephalic Sulf2-deficient mice in the first generations was about 35%. Up to the eighth generation of Sulf2-deficient mice the occurrence of a hydrocephalus was reduced to 10–15% of newborns. Hydrocephalic Sulf2-deficient mice were not only observed in the mouse line with hybrid C57BL/6 × 129 ola background used in this study, but further in an additional Sulf2-deficient mouse line with 129 ola background (see Methods, data not shown).

A congenital hydrocephalus normally develops due to either (*i*) impaired cerebrospinal fluid (CSF) flow (*hydrocephalus occludens*), (*ii*) reduced CSF reabsorption, (*iii*) excessive CSF production or (*iv*) a reduction in brain mass during neuronal development caused by deficits in neurite outgrowth, cell survival or migration

Fig. 1 Sulf2-deficient mice develop a congenital hydrocephalus. Coronal sections of juvenile wild-type (**A, D, E, H, L**) and Sulf2-deficient hydrocephalic mice (**B, C, F, G, I–K, M**) were stained with haematoxylin and eosin and examined by light microscopy. Sulf2 knockout mice showed a deformation of the nasal septum compared to age-matched control animals (**A, B**). The observed hydrocephalus was combined with an overall enlargement of the ventricle system, in particular the olfactory ventricle (ov) and the lateral ventricles (lv) (**C, F**). Coronal sections of Sulf2-deficient brains (**G**) showed a corpus callosum (cc) agenesis (compare G with E). In Sulf2-deficient hydrocephalic mice (**I**), a deformation of the hippocampus (hc) was detectable compared to age-matched wild-type animals (**H**). In comparison to control mice (**H, L**), the cortex (ct) of mutant mice (**J, K, M**) was reduced (ac, anterior commissure), in particular a reduction of deeper cerebral cortical layers was detectable (I–VI: lamina I–VI).

© 2008 The Authors
Journal compilation © 2009 Foundation for Cellular and Molecular Medicine/Blackwell Publishing Ltd

(*hydrocephalus ex vacuo*) [28]. To analyse the characteristics of the hydrocephalus caused by the lack of Sulf2, paraffin embedded brain sections from hydrocephalic Sulf2-deficient mice and age-matched wild-type animals were stained with haematoxylin and eosin and examined by light microscopy (Fig. 1). Coronal sections revealed a number of abnormalities in brains of Sulf2-deficient mice: The chondral anlage of the nasal septum was deformed, obviously as a consequence of the higher hydrostatic pressure before ossification (Fig. 1, compare A and B). In general, a deformation of the nasal septum agrees with the assumption that the hydrocephalus is a consequence of foetal malformations and thus is already present at birth. Furthermore, there was an obvious reduction of overall brain size detectable in all analysed hydrocephalic Sulf2-deficient mice which was combined with a general enlargement of the whole ventricle system, in particular the olfactory ventricles (Fig. 1C), the lateral ventricles (Fig. 1, compare F and D), the foramen interventriculare and the third ventricle (data not shown). In all analysed animals an open aquaeductus cerebri, which is the narrowest site of the ventricle system, excludes a *hydrocephalus occludens* (data not shown). Although Sulf2 is expressed in the plexus choroideus during neuronal development (Table 1), electron microscopic investigations of the plexus choroideus showed no obvious abnormalities giving no indication for an abnormal development of the CSF producing organ (data not shown). In general, in all analysed hydrocephalic mutants the cortex was thinner. Detailed analysis showed a reduction of deeper cerebral cortical layers (Fig. 1, compare D, L with F, M) which is in line with a Sulf2 characteristic expression pattern in the cortex anlage during embryogenesis and highest expression levels in lamina III, V and VI in adult mice (Table 1) [17, 29, 30]. In some dramatic cases the cortex was interrupted (Fig. 1J and K). Further severe malformations were found in all affected Sulf2-deficient mice showing an agenesis of the corpus callosum (Fig. 1, compare D, E with F, G). In addition, a deformation of the hippocampus was observed (Fig. 1, compare H and I). In conclusion, the results of the histological analysis of Sulf2 hydrocephalic mice reveal a reduction in brain mass during neuronal development characterized mainly by a corpus callosum agenesis and a thinner cortex, which allow us to classify the observed congenital hydrocephalus in Sulf2-deficient mice as *hydrocephalus ex vacuo* similar to the already described hydrocephalus for knockout mice lacking the neuronal cell adhesion molecule L1 [31].

Unaffected Sulf2-deficient mice show a normal histoarchitecture of the brain

Sulf2 is ubiquitously expressed in the developing and the adult nervous system with highest levels in the CA3 region of the hippocampus, the deeper cortical layers and the granular layer of the cerebellum (Table 1) [17, 29, 30]. However, histological analysis of inconspicuous Sulf2-deficient mice revealed no apparent neuroanatomical malformations in comparison to wild-type animals (Figs S1 and S2). Nissl stainings showed that all cortical layers are formed normally with a thickness indistinguishable from that of wild-type mice (Fig. S1 A and C). Furthermore, neither light microscopic analysis of the hippocampus nor Timm's staining of mossy fibres revealed any abnormalities in unaffected Sulf2 mutant mice (Fig. S1, compare D, G and F, I). Neurofilament L (Fig. S1 J and L), astrocyte-specific GFAP (glial fibrillary acidic protein) (Fig. S1 M and O) and presynaptic characteristic synaptophysin (data not shown) immunoreactivity were indistinguishable from that of wild-type mice. Also, Nissl stainings of the cerebellum of Sulf2-deficient mice (Fig. S2, compare A, D and C, F) as well as cerebellar Neurofilament L (Fig. S2 G and I), GFAP (Fig. S2 J and L) and synaptophysin (data not shown) immunoreactivity appeared histologically normal despite a broad expression of Sulf2 in the granular layer. In addition, detailed analysis of major brain commissures showed no light microscopic abnormalities (data not shown).

To summarize, microscopic analysis of the cerebellar cortex, hippocampus and cerebellum of unaffected adult Sulf2-deficient mice showed a normal histoarchitecture. Nevertheless, the observed results of the histological analysis of Sulf2 hydrocephalic mice clearly support the hypothesis that Sulf2 is involved in the development of the murine central nervous system.

To address the question as to whether the observed histological deficits in Sulf2 hydrocephalic-deficient mice are based exclusively on developmental deficits or a combination of an impaired development and additional acute effects in the adult nervous system, further detailed analyses were performed.

Developmental malformations in Sulf2-deficient mice lead to enhanced embryonic lethality

To analyse whether developmental, in particular the neuroanatomical malformations presenting at birth for the hydrocephalic mice (see above) can also explain the higher embryonic lethality of Sulf2-deficient embryos, we examined 49 mutant embryos at embryonic day 12.5. Indeed, eighteen of them showed developmental malformations. In six cases we found resorption of the embryo before embryonic day 12.5 (Fig. 2H). Most of the observed defects affected the development of the nervous system. Malformed embryos showed a reduced size of all brain vesicles, in particular of the rhombencephalon, which was sometimes combined with neural tube closure defects at the level of the mesencephalic or telencephalic vesicles (Fig. 2B and C). Closure defects of the cranial neural tube during neuronal development are often associated with a congenital hydrocephalus [32]. Furthermore, in some Sulf2 mutants dramatic malformations of the whole embryo were found where the characteristic patterning of the brain vesicles was completely absent (Fig. 2E–G). Interestingly, the observed malformations confirm the expression pattern of Sulf2 in the developing nervous system with highest levels detectable in the hindbrain, midbrain and telencephalic vesicle [17, 29, 30]. Based on the results of the light microscopical studies of Sulf2 hydrocephalic mice and the analysis of Sulf2 mutants at

© 2008 The Authors
Journal compilation © 2009 Foundation for Cellular and Molecular Medicine/Blackwell Publishing Ltd

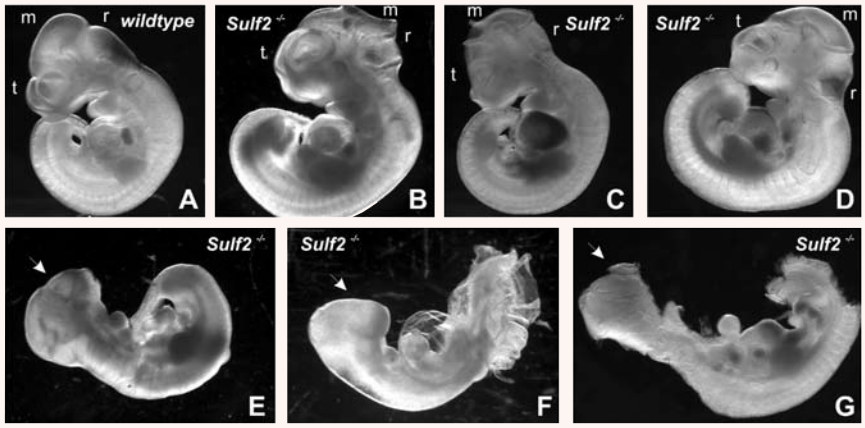

H

	normal	resorbed	malformed	total
embryos at E 12.5	31 (**63 %**)	6 (**12 %**)	12 (**24 %**)	49

Fig. 2 Developmental malformations in Sulf2-deficient embryos at embryonic day 12.5. At embryonic day 12.5, mouse foetuses deficient in Sulf2 (**B–G**) showed serious developmental malformations, in particular malformations of the central nervous system compared to age-matched wild-type embryos (**A**). Affected mutant embryos were characterized by reduced size of the telencephalic (t), mesencephalic (m) and, in particular, rhombencephalic (r) brain vesicles (**B–D**), in some cases combined with an open neural tube at the level of the mesencephalon (**B, C**) or telencephalon (**C**). In embryos with more dramatic malformations, the normal patterning of the cranial neural tube was completely absent (**E–G**, arrows). (**H**) Statistical analysis of 49 examined Sulf2-deficient embryos.

embryonic day 12.5 we conclude that the lack of Sulf2 enzyme function results in developmental malformations, in particular of the brain, which lead to higher embryonic lethality or, in less progressive cases, to congenital hydrocephalus.

Sulf1-deficient mice show no neuroanatomical malformations

Expression studies at the mRNA level detect similar amounts of Sulf1 and Sulf2 transcripts in the developing nervous system but not at adult stages (Table 1). However, despite a ubiquitous expression during development no neuronal malformations were observable in adult Sulf1-deficient mice; histological analysis revealed no brain patterning defects (Figs S1 and S2). Nissl stainings of cerebral cortical layers revealed no abnormalities compared to wild-type animals (Fig. S1 A and B). Additionally, light microscopically analysed Sulf1-deficient hippocampi were indistinguishable from that of control mice (Fig. S1 D and E). No differences were detectable in Timm's stainings of mossy fibres (Fig. S1 G and H) or in Neurofilament L (Fig. S1 J and K), GFAP (Fig. S1 M and N) and synaptophysin (data not shown) immunoreactivity. Also, light microscopical (Fig. S2, compare A, D and B, E) and immunohistochemical analysis (Fig. S2, compare G, J and H, K) of the cerebellum of Sulf1-deficient mice displayed no abnormalities. Furthermore, no differences in major brain commissures were detectable using light microscopical methods (data not shown).

Sulf1- and Sulf2-deficient cerebellar and hippocampal neurons show a decrease in neurite length

The results of the histological analysis of Sulf2 hydrocephalic mice displayed a reduction in brain mass. The compensatory enlargement of the ventricle system in response to loss of brain parenchyma, as observed for affected Sulf2-deficient mice, is defined as *hydrocephalus ex vacuo* (see above). Since we could not find any obstruction of the ventricle system and abnormalities of the plexus choroideus, the question arose whether Sulf2 dependent defects in neuronal development are based on neurite outgrowth deficits, which could further explain the observed corpus callosum agenesis and reduction in cerebral cortex thickness.

To investigate this hypothesis, neurite outgrowth of cerebellar microexplants and hippocampal single cell cultures was analysed. We focused on these two brain areas as both sulfatases are expressed differentially in the cerebellum and hippocampus during neuronal development and in the adult nervous system (Table 1). Cerebellar microexplant cultures isolated from wild-type, Sulf1- or Sulf2-deficient mice were maintained on poly-L-lysine or on a combination of poly-L-lysine and laminin (Fig. 3A).

We chose poly-L-lysine as a non stimulating substrate and laminin as a neurite outgrowth promoting extracellular matrix molecule. Although no histological abnormalities were detectable in Sulf1-deficient adult mice, surprisingly explants isolated from Sulf1 mutant mice maintained on poly-L-lysine as well as on the

© 2008 The Authors
Journal compilation © 2009 Foundation for Cellular and Molecular Medicine/Blackwell Publishing Ltd

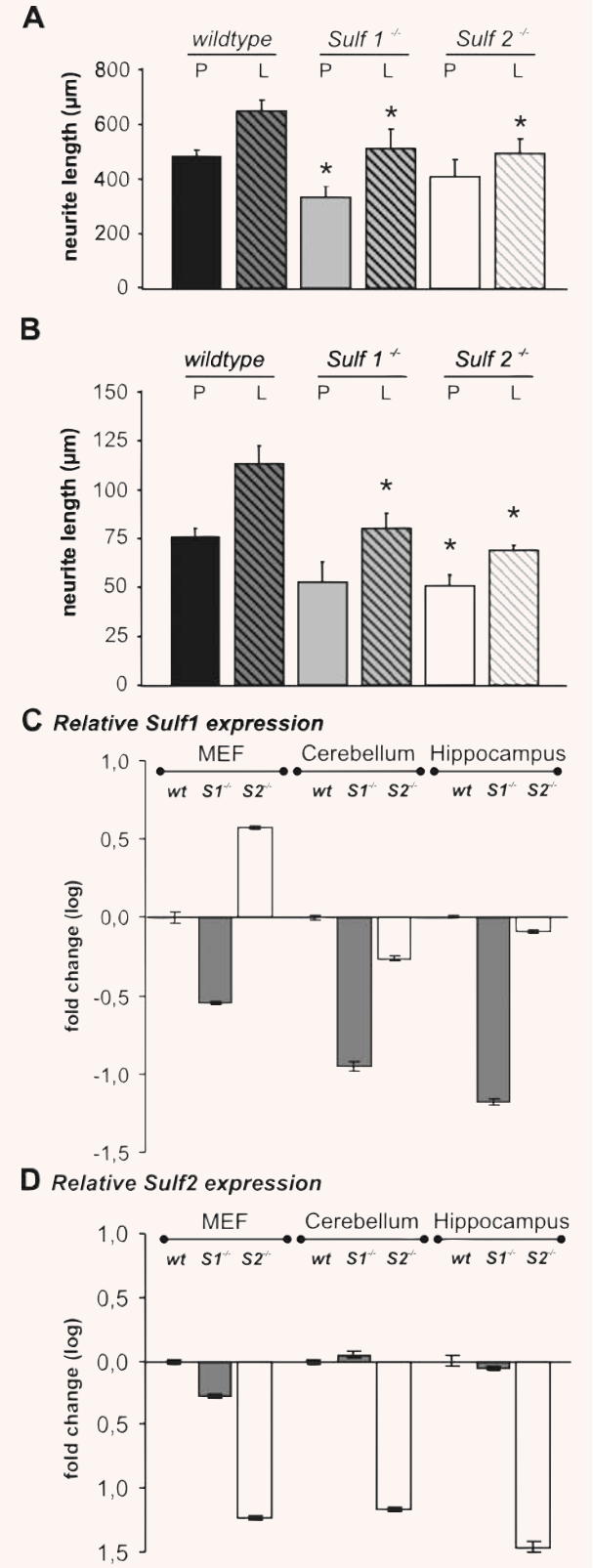

substrate combination poly-L-lysine plus laminin showed a clear reduction in neurite length (Fig. 3A). Likewise laminin dependent neurite outgrowth of Sulf2-deficient cerebellar explants was significantly reduced (Fig. 3A). In contrast, Sulf2-deficient explants on poly-L-lysine showed no significant difference in neurite length compared to wild-type explants (Fig. 3A).

Axon outgrowth towards specific targets is dependent an guidance cues in the extracellular matrix as well as on the cell surface of neighbouring cells which modulates dynamic changes in the polymerization of cytoskeletal filaments. To analyse whether the observed deficits in neurite outgrowth of Sulf1- and Sulf2-deficient cerebellar explants can be explained by an altered growth cone morphology, phalloidin stainings of explant cultures were investigated using fluorescence microscopy (data not shown). Neither Sulf1- nor Sulf2-deficient growth cones from cerebellar explants were morphologically distinguishable from that of wild-type mice. Growth cones were well elaborated with filopodial and lamellipodial structures.

Furthermore, analysing the neurite lengths of isolated hippocampal single cell cultures, using the same substrates as above, revealed a decrease in neurite length on poly-L-lysine and a much more pronounced reduction in neurite length on a combination of the substrates poly-L-lysine and laminin for neurons of both Sulf1- and Sulf2-deficient mice in comparison to wild-type neurons (Fig. 3B). Phalloidin stainings of hippocampal neurons revealed no differences in growth cone morphology between wild-type and Sulf1-deficient neurons (data not shown). In contrast, Sulf2-deficient hippocampal neurons showed a slightly altered growth cone morphology as they appear smaller and the typical hand-shaped structure was often missing (data not shown). Further detailed analysis concerning filopodia number

Fig. 3 Effect of Sulf1 and Sulf2 deficiency on neurite outgrowth of cerebellar and hippocampal neurons. (**A**) Cerebellar microexplant cultures from wild-type, Sulf1- and Sulf2-deficient mice (postnatal day 6) were plated onto glass coverslips coated with poly-L-lysine (PLL) (P) or a combination of PLL and laminin (L). After incubation for 48 hrs at 37°C explants were fixed and stained. Neurite outgrowth from the explants was quantitated by measuring the length of the 10 longest neurites of 10 aggregates in three independent experiments. (**B**) A similar analysis was performed for hippocampal neurons (postnatal day 1). Neurite outgrowth was quantitated after 48 hrs by measuring the length of 100 neurites in three independent experiments; the *asterisks* indicate statistically significant differences of Sulf-deficient neurons as compared to wild-type neurons ($P < 0.05$). (**C, D**) The expression of Sulf enzymes were investigated by real-time PCR analysis using mRNAs from Sulf1 ($S1^{-/-}$), Sulf2 ($S2^{-/-}$) deficient and wild-type (wt) mouse embryonic fibroblasts (MEF), cerebellar (Cerebellum) and hippocampal (Hippocampus) neurons. (**C**) Whereas Sulf1 mRNA was up-regulated in Sulf2-deficient MEFs, a compensatory increase in expression levels of Sulf1 was not detectable for Sulf2-deficient cerebellar and hippocampal neurons. (**D**) Furthermore, an increase in expression of Sulf2 in Sulf1-deficient mRNA samples was not detectable. The fold change for Sulf1 and Sulf2 was calculated relative to the wild-type control. The house-keeping gene RPL was used to normalize the mRNA of each sample relative to each other. Results are expressed as means ± S.D.

© 2008 The Authors
Journal compilation © 2009 Foundation for Cellular and Molecular Medicine/Blackwell Publishing Ltd

and filopodia elongation will be necessary to characterize this defect in detail.

Taken together, these *in vitro* data demonstrate that loss of either Sulf1 or Sulf2 function leads to a decrease in neurite length in cerebellar and hippocampal neurons. These results are on one hand in line with the ubiquitous expression pattern of Sulf1 and Sulf2 in the developing nervous system; on the other hand they cannot explain the inconspicuous histological analysis of Sulf1 and unaffected Sulf2-deficient adult mice.

In vitro phenotypes are sulfatase-specific

As real-time PCR analysis of mouse embryonic fibroblasts isolated from Sulf1- and Sulf2-deficient mice had revealed an up-regulation of Sulf1 expression in Sulf2-deficient fibroblasts [13], overlapping functions of Sulf1 and Sulf2 were suggested. To analyse whether the observed neurite length reduction of Sulf1- and Sulf2-deficient cerebellar granule and hippocampal cells is accompanied by an up- or down-regulation of Sulf1 in the Sulf2 knockout situation, or *vice versa*, we investigated the expression levels of Sulf1 and Sulf2 in cerebellar and hippocampal single cell cultures in comparison to mouse embryonic fibroblasts (Fig. 3C and D). Surprisingly, different from the situation in MEFs neither an up-regulation of Sulf1 in Sulf2-deficient cerebellar and hippocampal neurons (Fig. 3C) nor a compensatory expression of Sulf2 in Sulf1-deficient cells were detectable (Fig. 3D).

In conclusion, functional co-operativity of the Sulf enzymes as judged from co-reulgated expression seems to be cell-type-specific. Further, since no up-regulation of Sulf1 in the Sulf2 knockout or *vice versa* was observed, the described *in vitro* phenotypes are sulfatase-specific. In addition these results for the first time give additional information concerning Sulf1 and Sulf2 expression in the postnatal central nervous system, as real-time PCR results clearly show that Sulf1 and Sulf2 are expressed in primary cell cultures of the postnatal cerebellum (P6) and hippocampus (P1).

Unaltered basal synaptic transmission and LTP in Sulf2-deficient mice

The development of synaptic connections in the hippocampus is modulated by a number of factors, among them HSPG-dependent molecules like the neural cell adhesion molecule (NCAM) [33] or heparin-binding-growth associated molecule (HB-GAM) [34]. To investigate whether the observed reduction in neurite length of hippocampal neurons in both mutant strains *in vitro* and the described altered morphology of hippocampal growth cones of Sulf2-deficient mice result in altered neuronal connections in the hippocampus we analysed the basal synaptic transmission and LTP level of synapses between Schaffer collaterals and principal pyramidal neurons of the CA1 region in hippocampal slice preparations of Sulf2- and Sulf1-deficient animals.

One-month-old Sulf2-deficient mice show normal basal levels of excitatory transmission (Fig. S3 A and C). Stimulus-response curves for fEPSPs evoked by stimulation of Schaffer collaterals and paired-pulse facilitation measured at interpulse intervals between 10 and 200 ms, as a paradigm to assess presynaptic function [34, 35], were not different between Sulf2-deficient mutants and wild-type controls. Furthermore, the ratio between fEPSP amplitude and fibre volley was not significantly different between genotypes (Fig. S3 A). In addition, we investigated hippocampal synaptic plasticity. TBS of Schaffer collaterals reliably produced short-term potentiation (PTP) and LTP in slices from wild-type and Sulf2-deficient animals (Figs 4A and S3). There was no significant difference between the genotypes detectable. The lack of any phenotype in Sulf2-deficient juvenile mice led us to further analyse synaptic plasticity in 3-month-old adult Sulf2-deficient mice which are characterized by a completely developed hippocampus. Surprisingly, also in these mice no alterations in synaptic plasticity were observed (Fig. S3 E and G). In summary, Sulf2-deficient mice show no alterations in basal synaptic transmission and in synaptic plasticity in the CA1 area of the hippocampus. To further analyse the importance of Sulf2 function for the adult hippocampus additional electrophysiological studies should be done with the focus on the CA3 region of the hippocampus, where the highest expression levels of Sulf2 in adulthood were detectable [29, 30].

Unaltered basal synaptic transmission, but impaired LTP in Sulf1-deficient mice

Similar to Sulf2-deficient mice, no significant differences between Sulf1-deficient mutants and wild-type littermates at 1 month of age were found demonstrating normal basal levels of excitatory transmission and its presynaptic modulation (Fig. S3). Furthermore, the ratio between fEPSP amplitude and fibre volley was not significantly different between genotypes (Fig. S3 B, inset). In addition, we investigated hippocampal synaptic plasticity in Sulf1-deficient mice. TBS of Schaffer collaterals reliably produced short-term potentiation (PTP) and LTP in all slices measured from wild-type animals (Figs 4B and S3). No difference in the levels of PTP in Sulf1-deficient mice were measurable. On the contrary, TBS-induced LTP was significantly reduced (Fig. 4B), as compared to wild-type mice (Student's t-test, $P = 0.032$). In summary, in contrast to mice lacking Sulf2 function, Sulf1-deficient mice show normal basal synaptic transmission but an impairment of CA1 dependent Schaffer collateral LTP in the hippocampus.

Sulf1-deficient mice show a reduced hippocampal spine density

As histological analysis of Sulf1-deficient mice revealed no neuroanatomical malformations, the mechanisms of the Sulf1

© 2008 The Authors
Journal compilation © 2009 Foundation for Cellular and Molecular Medicine/Blackwell Publishing Ltd

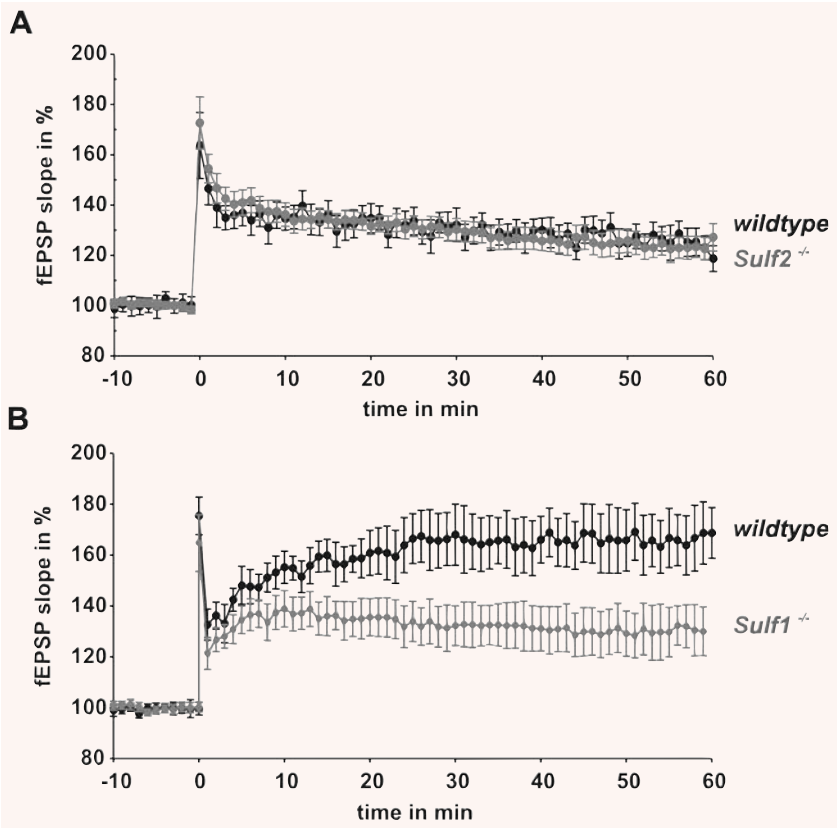

Fig. 4 Impaired LTP in 1-month-old Sulf1-deficient mice as compared to age-matched Sulf2-deficient and wild-type control mice. (**A**) TBS (theta burst stimulation) of Schaffer collaterals (applied at time point 0) evoked a similar increase in the slopes of fEPSPs recorded in the CA1 region of slices from wild-type and Sulf2-deficient mice. (**B**) In contrast, in slices from Sulf1-deficient mice, the potentiation appeared significantly lower than in wild-type littermates. The mean slope of fEPSPs recorded 0–10 min. before TBS was taken as 100%. Data represent mean ± S.E.M. (**A**: $n = 10$ for wild-type and $n = 10$ for knockout, **B**: $n = 7$ for wild-type and $n = 10$ for knockout); *n* indicates the number of tested slices.

characteristic deficits in LTP seem to be mediated on a molecular level. One possible cause of deficits in synaptic plasticity is an alteration in spine morphology or density. Dendritic spines in the stratum radiatum of the CA1 region of Sulf1-, Sulf2-deficient and wild-type mice were analysed using transmission electron microscopy (Fig. 5). Sulf1-deficient hippocampal neuron morphology was found to be in the normal range except for a markedly reduced frequency of dendritic spines (Fig. 5, compare A, B and C, D) and a synapse structure, in which both the postsynaptic density and the number of synaptic vesicles were reduced (Fig. 5D). Morphometrically, synapse counts in the stratum radiatum of the CA1 region were significantly reduced (Student's t-test, $P < 0.001$) with 0.18 (± 0.06) synapses per μm^2 in Sulf1-deficient animals compared to 0.38 (± 0.1) in the wild-type and 0.33 (± 0.09) synapses per μm^2 in Sulf2-deficient mice. Furthermore, in contrast to Sulf1-deficient mice, the number and density of dendritic spines in the hippocampal CA1 region of Sulf2-deficient mice were indistinguishable from that of control mice (Fig. 5, compare A, B and E, F).

Taken into account that (*i*) Sulf1 expression in the hippocampus is limited to the early developing nervous system in the dorsal telencephalic vesicle [16], which gives rises to the later hippocampal anlage [36], and (*ii*) the expression of the enzyme is not detectable in the adult hippocampus we conclude that the impaired LTP combined with a reduction in spine density result from developmental and not from acute defects.

Behavioural alterations in Sulf1- and Sulf2-deficient mice

LTP, which is impaired in Sulf1-deficient animals, is a long lasting augmentation of synaptic strength that has been suggested as a cellular mechanism underlying specific learning and memory processes. Therefore, behavioural characteristics of Sulf1- and Sulf2-deficient mice were compared to those of wild-type controls at 3 months of age. Our extended behavioural battery comprised tests for neuromotor ability and activity, emotionality and anxiety, and learning and memory. Defects were observed in neuromotor and learning performance in both mutant groups but the extent and pattern of the alterations were again different between Sulf1- and Sulf2-deficient mice.

The neuromotor tests included rotarod, grip strength and cage activity recordings. During 4 consecutive rotarod trials, the time was recorded that mice were able to stay on the accelerating rotating rod. No significant genotype difference was found during these trials (data not shown). The grip strength test did show reduced readouts for Sulf2-deficient mice (345 ± 21 mN, $P < 0.001$)

© 2008 The Authors
Journal compilation © 2009 Foundation for Cellular and Molecular Medicine/Blackwell Publishing Ltd

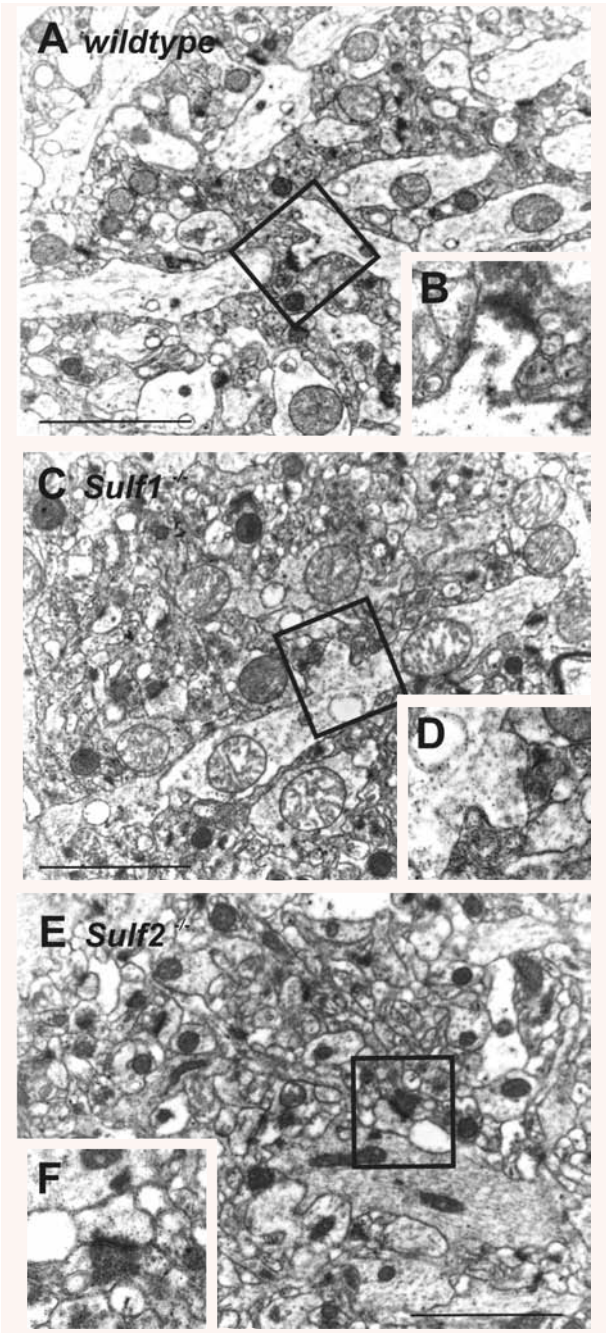

Fig. 5 Reduced spine density in 3-month-old Sulf1-deficient mice. Representative transmission electron microscopy images from the stratum radiatum of the hippocampal CA1 region of wild-type (**A, B**), Sulf1 (**C, D**) and Sulf2 (**E, F**) knockout mice taken at 22, 500× (A, C, E) and 55,000× (B, D, F) magnification. High magnification shows that Sulf1-deficient mice had fewer dendritic spines which, in addition, showed reduced postsynaptic densities and synaptic vesicle numbers (**D**). Scale bars: 1 μm (**A, C, E**).

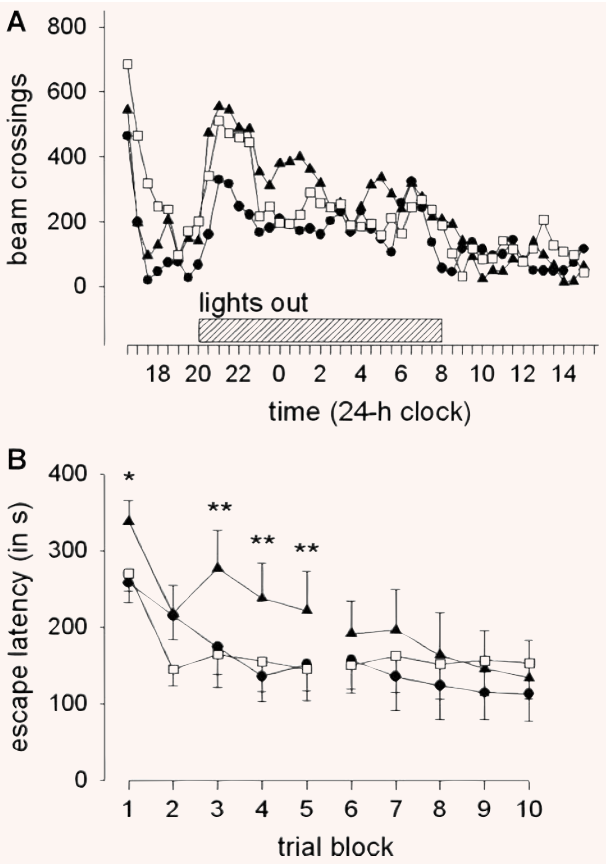

Fig. 6 Behavioural differences between 3-month-old Sulf1- and Sulf2-deficient mice and wild-type controls. The 24-hr cage activity profile shows that nocturnal perambulation (lights are out between 8 pm and 8 am) was decreased in Sulf1-deficient mice (**A**). However, the exploratory activity peak (between 16:30 and 19:00) was decreased in Sulf1 as well as Sulf2-deficient mice. During the first trial blocks of water maze training (**B**), escape latency was significantly increased in Sulf2-deficient mice compared to wild-type controls. Sulf1-deficient mice also displayed a slightly decreased slope, but the defect was less pronounced compared to Sulf2-deficient mice. Both plots show mean values for wild-type mice (open squares), Sulf1-deficient (closed circles) and Sulf2-deficient mice (closed triangles). *Asterisks* indicate significance of differences from control values in *post hoc* pairwise comparison (Fisher LSD): $*P < 0.05$, $**P < 0.01$.

compared to Sulf1-deficient (453 ± 16 mN) and wild-type mice (425 ± 17 mN).

Cage activity recordings showed a stable and typical pattern in wild-type mice with an exploratory peak when they were introduced in the recording cages, and intense nocturnal perambulation (Fig. 6A). Notably, activity recordings were quite different in Sulf1- and Sulf2-deficient mice with a significant effect of genotype ($P = 0.02$, RM-ANOVA). Twenty-four hours of activity patterns were quite different between the genotypes (significant effects of genotype × time interaction, $P < 0.001$). Sulf1-deficient

© 2008 The Authors
Journal compilation © 2009 Foundation for Cellular and Molecular Medicine/Blackwell Publishing Ltd

mice ($P < 0.05$, Fisher LSD) displayed reduced nocturnal perambulation compared to Sulf2-deficient and wild-type mice. It is also interesting to note that the exploration peak upon introduction into the recording cages was reduced in both Sulf1- and Sulf2-deficient mice.

Emotionality and anxiety were assessed in the elevated plus maze, open field and social exploration tests (data not shown). None of the exploratory conflict measures showed any significant effect of genotype. For example, the typical anxiety measure in elevated plus maze exploration (*i.e.* percentage of time spent in the open arms) was quite similar in the different groups ($F_{2, 42} = 0.36$, $P = 0.5$) with 22.0 $\pm$ 3.0% in wild-type mice, 25.6 $\pm$ 2.7% in Sulf1-deficient, and 25.3 $\pm$ 2.6% in Sulf2-deficient mice.

Passive avoidance learning was also not different between the genotypes, but spatial learning performance in the Morris water maze clearly was (Fig. 6B). Mice were trained for 2 weeks in the maze, followed by probe trials without a platform present. Differences in escape latency and path length were observed during the training. Acquisition started somewhat slower in Sulf1-deficient mice, which required 3 trial blocks to reach asymptotic performance (compared to 2 trial blocks in controls), but it was markedly slowed in Sulf2-deficient mice that showed consistently longer escape latencies than controls during nearly all training trials (Fig. 6B). In fact, genotype significantly affected escape latency ($P = 0.001$; RM-ANOVA) with Sulf2-deficient mice showing much worse performance compared to wild-type as well as Sulf1-deficient mice ($P < 0.05$, Fisher LSD). The three genotype groups did eventually reach similar performance with extended training (trial blocks 6 to 10). Consequently, the probe trials (not shown) that were performed after 10 training trials, did not demonstrate any genotype effect.

Discussion

Specific and/or overlapping functions of Sulf1 and Sulf2 in the developing nervous system

The sulfation patterns of HS chains present important signalling determinants. In particular, 6-O-sulfate groups have been shown to influence signal transduction processes. Sulf1 and Sulf2 are able to cleave specific 6-O-sulfate groups within the HS chain, thereby changing sulfation patterns and affecting signalling processes, many of which with key relevance for developmental tissue patterning. *In vitro* studies have shown that Sulf1 is involved in mesoderm formation and angiogenesis by inhibiting FGF-2 and FGF-4 signalling [23]. Furthermore, Sulf1 modulates Sonic hedgehog (Shh) signal transduction processes in the ventral spinal cord [37] and is involved in cartilage and joint development [22, 38]. Additionally, it has been shown that Sulf1 expression is necessary for normal vascular smooth muscle cell proliferation, migration and cell death [39]. As these *in vitro* studies implicate an important role for Sulf1 function in development, the lack of an overt phenotype, at first sight, in the Sulf1-deficient mouse strain was surprising. This result agrees with the phenotypical analysis of an inconspicuous Sulf1 gene-trap mouse, recently described by Holst *et al.* [16]. Since neither the Sulf1 nor the Sulf2 gene-trap mice showed any overt phenotype, whereas double knockout mice were characterized by highly penetrant neonatal lethality, the authors proposed a redundancy of both enzymes. This hypothesis was partially supported by the observation that in embryonic fibroblasts, isolated from our Sulf2 knockout mice, Sulf1 expression was up-regulated as determined at mRNA level [13]. Although *vice versa* no overexpression of Sulf2 in Sulf1 knockout mouse embryonic fibroblasts was detectable [13], the lack of an overt phenotype in Sulf1-deficient mice could in principle be explained by compensation through Sulf2. On the contrary, in this study we could show that different from the situation in mouse embryonic fibroblasts no up-regulation of Sulf1 in Sulf2-deficient cells or *vice versa* was detectable through real-time PCR analysis using mRNAs from primary cerebellar and hippocampal cultures (Fig. 3). Furthermore the total knockout of Sulf2 function, as described here, results in neuroanatomical malformations leading to higher embryonic lethality. This contrasts with the rather mild phenotypes of the described Sulf2 gene-trap mouse lines [16, 17]. The importance of Sulf2 function for neuronal development is further reflected by the observed congenital hydrocephalus in Sulf2-deficient newborns with frequencies of up to 35% in the first knockout generations. The decreasing penetrance of hydrocephali in Sulf2-deficient mice with increasing generation number may be due to modifier genes. Similar observations were made for other HS modifying enzymes when knocked out in mice, *e.g.* N-deacetylase/N-sulfotransferase-1, heparan sulfate-3-O-sulfotransferase-1 or heparan sulfate-2-O-sulfotransferase-deficient mice, which display either non-penetrant phenotypes and/or variable expressivity [40–42]. Although affected Sulf2-deficient mice bearing a hydrocephalus represent only a relatively small fraction of animals, the penetrance is significantly increased in comparison to the naturally occurring hydrocephalus in 1–4% of wild-type C57Bl/6 inbred mice which were used in combination with 129 ola mice as genetic background for the generation of Sulf2-deficient animals (The Jackson Laboratory, http://jaxmice.jax.org/strain/000664.html).

The described phenotype in this classical knockout situation clearly argues against the hypothesis of a general redundancy of the Sulf enzymes. A possible explanation for the explicit difference in Sulf1 and Sulf2 knockout mice could be due to partial non-overlapping expression of Sulf2, as previously described [17], in critical areas of the developing nervous system. Indeed, the specific neurological deficits in Sulf2-deficient mice indicate that certain processes during the development of the nervous system are exclusively mediated by Sulf2 function. However, whether the inconspicuous phenotype of Sulf1-deficient mice or the developmental deficits of Sulf2-deficient mice are sulfatase-specific or further influenced by functional co-operativity of both enzymes should be carefully analysed for different developmental stages, brain areas and cell-types.

© 2008 The Authors
Journal compilation © 2009 Foundation for Cellular and Molecular Medicine/Blackwell Publishing Ltd

Like Sulf1, also Sulf2 can modulate various growth factor signalling pathways *in vitro* affecting vascular endothelial growth factor (VEGF), FGF-1, SDF-1, Wnt and FGF-2 dependent processes [13, 21, 43]. The interaction between FGF-2 and fibroblast growth factor receptor-1 (FGFR-1) requires ternary complex formation involving HS 6-O-sulfate groups [44, 45]. The finding that FGFR-1-deficient mice display neural tube defects similar to those observed in Sulf2-deficient mice [46] is highly suggestive of an *in vivo* implication of Sulf2 in FGF2 mediated signalling processes during the development of the nervous system. Consistently, FGF2 knockout mice further show an overall reduction and defects in the organization of cerebral cortical layers [47], a phenotypical attribute also presented by Sulf2-deficient hydrocephalic mice. Unfortunately nothing is known about the *in vivo* proteoglycan specificity of the Sulf enzymes. Perlecan represents a substrate candidate for Sulf2, as perlecan knockout mice are characterized by dramatic cephalic malformations, in particular by brain atrophy in telencephalic areas [48, 49].

Neuroanatomical malformations, like neural tube closure defects or hydrocephali, as observed in our Sulf2-deficient mice, are often based on proliferation, apoptosis, migration or neurite outgrowth defects which result in brain atrophy, as had been described for the knockout of the neural cell adhesion molecule L1 [31]. In fact, an overall reduction in neurite length of Sulf2-deficient cerebellar explants and hippocampal neurons was detectable. Surprisingly, however, also neurons isolated from Sulf1-deficient mice exhibited a significant reduction in neurite length. For both Sulf knockouts this was clearly seen for laminin-dependent neurite outgrowth, which had earlier been shown to involve HSPGs, *e.g.* syndecan-2 and -4, or HS binding factors such as HB-GAM [50–52]. Under the influence of Sulf deficiency differential 6-O-sulfation patterns of HS side chains could eventually promote or inhibit the interaction of HSPGs with laminin and their receptors, the integrins, thereby triggering intracellular signal transduction processes, which further modulate axon outgrowth.

Such outgrowth deficits, observed for both Sulf1- and Sulf2-deficient neurons *in vitro*, are likely the cause of the observed Sulf2-specific neuroanatomical phenotype which appears to be significantly compensated in the Sulf1 knockout mouse. It may however be possible that at earlier embryonic stages a delayed brain development can be traced for both Sulf1- and Sulf2-deficient embryos. This hypothesis is currently under investigation. Indeed, a markedly reduced spine density in the CA1 region of the hippocampus was detected in Sulf1 knockouts. This, in combination with the Sulf1 characteristic neurite outgrowth deficit, leads us to conclude that Sulf1 is also involved, though not essentially, in the development of the murine nervous system. Further, as HS sulfation state and proteoglycan type have been shown to influence neural development [10], it will be interesting to analyse the correlation between HS sulfation patterns, specific HSPG subtypes such as agrin or glypican-2 which are known to modulate axon outgrowth [53, 54], and HS-binding growth factors like FGF-2, GDNF, Shh or SDF-1 [13, 15, 16, 23, 43], which may help explain specific pathophysiological phenotypes observed in the Sulf knockouts.

Sulf1 and Sulf2 in the adult nervous system

In the adult nervous system HSPGs accumulate in the extracellular space between pre- and postsynapses, thereby modifying various aspects of synaptic differentiation, maturation and in particular their plasticity [55]. Especially the significance of sulfate groups of HSPGs, the substrates of both sulfatases, for the LTP of Schaffer collaterals in the CA1 region of the hippocampus has been proven by the *in vitro* finding that the inhibitory effect of heparin on LTP is dependent on specific sulfation patterns of the HS chain, namely iduronate-2-O-sulfate and glucosamine-6-O-sulfate [56]. The impairment of LTP in Sulf1-deficient mice clearly supports these results, although the molecular mechanism seems to be developmental and not an acute effect. Notably, Sulf1 is not detectable in the adult hippocampus. Thus it appears to be the lack of enzyme function during earlier embryonic stages that disturbs spine development in the CA1 region (Fig. 5) resulting in an impaired synaptic plasticity (Fig. 4). Surprisingly, impairment of LTP was not detectable in Sulf2 knockouts, although age-matched Sulf2-deficient mice do show marked spatial learning deficits. We conclude that behavioural deficits in Sulf2 knockouts arise from the impairment of developmental processes other than synapse development, or from acute defects in brain regions other than hippocampus. This is feasible, as Sulf2 is ubiquitously expressed in the adult central nervous system. For example, cerebellar defects may also lead to impaired water maze performance in mice [57].

The importance of HSPGs for synaptic transmission has been confirmed by studies in mice lacking or overexpressing HSPGs or HSPG-dependent proteins. Such mouse models display various deficits in neuronal and behavioural plasticity; *e.g.* syndecan-3 knockout mice are characterized by an increase in LTP, impaired spatial memory and reduced context dependent freezing [58]. Furthermore, mice overexpressing HB-GAM show a decrease in LTP, faster learning in Morris maze and decreased anxiety in elevated plus-maze [59]. The fact that the observed phenotypes in our Sulf knockouts on the one hand partially overlap with those of, *e.g.* syndecan-3-deficient or HB-GAM-overexpressing mice, but fail to exhibit defects in emotion and anxiety, supports the idea that the function of the Sulf enzymes and the protein expression of their HSPGs substrates are temporally and spatially regulated.

Finally, behavioural analysis revealed a reduction in grip strength for Sulf2-deficient mice. Whether the enzyme directly participates in muscle fibre generation or neuromuscular junctions fail to establish, as recently shown for oesophageal innervation in Sulf1 and Sulf2 double knockout mice [15], remains an open question. However, syndecan-3 and syndecan-4 represent substrate candidates during skeletal muscle development [60].

Conclusion

The 6-*O*-endosulfatases Sulf1 and Sulf2, which have an overlapping expression pattern in the developing nervous system, are

© 2008 The Authors
Journal compilation © 2009 Foundation for Cellular and Molecular Medicine/Blackwell Publishing Ltd

Table 2 Phenotypical characteristics of Sulf1- and Sulf2-deficient mice

	Sulf1-deficient mice	Sulf2-deficient mice
General		Reduced body weight
		Enhanced embryonic lethality
Developing nervous system		
		Congenital hydrocephalus
	Impaired neurite outgrowth (*in vitro*)	Impaired neurite outgrowth (*in vitro*)
Adult nervous system		
	Impaired LTP (CA1 region)	
	Reduced spine density (CA1 region)	
	Reduced nocturnal perambulation	
		Impaired spatial learning (increased Escape latency in MWM)
		Reduced grip strength

both involved in specific developmental processes of the brain (for summary, see Table 2). In contrast to Sulf1, its homologue Sulf2 is required for the development of the murine central nervous system, although obviously compensatory mechanisms exist. Whether the rather mild phenotype of Sulf1-deficient mice is due to functional overlap of both sulfatases has to be further clarified. Sulf1 and Sulf2 are differentially involved also in neuronal and behavioural plasticity of the adult nervous system. Taken together, the described phenotypes are specific for each sulfatase which leads to the conclusion that both sulfatases fulfil functionally distinct roles during neural development and in the adult nervous system. The complexity and spatial-temporal specificity of the observed phenotypes argue in favour of a functional co-operativity of both enzymes, although a limited redundancy cannot be excluded.

Acknowledgements

We would like to thank Kerstin Böker, Nicole Tasch, Leen Van Aerschot, Anke Schönherr, Irmgard Weiß, Marion Knufinke and Christiane Grebe for excellent technical assistance. Further, we are grateful to Renate Lüllmann-Rauch (Department of Anatomy, University of Kiel) for initial histological analysis, Peter Schwartz (Department of Anatomy and Embryology, University of Göttingen) for electron microscopy, and to William C. Lamanna for critically reading the manuscript.

Supporting Information

The following supporting information is available for this article:

Figure S1. Morphology of the cortex and the hippocampus of Sulf1- and Sulf2-deficient mice. Light microscopic analysis of the cerebellar cortex (**A**–**C**) and the hippocampus (**D**–**F**) of 3-month-old Sulf1 (**B, E**) and Sulf2 (**C, F**) deficient mice demonstrated an apparently normal histoarchitecture of these CNS structures compared to wild-type mice (**A, D**) (cerebellar cortex: 100×, hippocampus: 25×), (I–VI: lamina I–VI). Timm's staining of the hippocampus revealed a similar laminated organization of the CA3 subfield in wild-type (**G**), Sulf1 (**H**) and Sulf2 (**I**) deficient mice (25×). Double-label immunofluorescence to detect Neurofilament L (**J**–**L**) and GFAP (glial fibrillary acidic protein) (**M**–**O**) showed that the neuron-specific intermediate filament Neurofilament L immunoreactivity (**J**–**L**) is not detectably altered in the CA1 region of the hippocampus of Sulf1 (**K**) and Sulf2 (**L**) deficient mutants (630×). Also the astrocyte-specific marker GFAP (**M**–**O**) showed a normal distribution in the CA1 region of Sulf1 (**N**) and Sulf2 (**O**) mutant mice (630×). Sections **J**–**O** were counterstained with DAPI (**P**–**R**); SP, stratum pyramidale; SO, stratum orientale; SR, stratum radiatum.

Figure S2. Cerebellar morphology of 3-month-old Sulf1- and Sulf2-deficient mice. Light microscopic analysis of the cerebellum of Sulf1 (**B, E**) and Sulf2 (**C, F**) deficient mice demonstrated an apparently normal histoarchitecture of the Molecular (ML), Granular (GL) and Purkinje (PL) layer compared to wild-type mice (**A, D**) (**A**–**C**: 25×, **D**–**F**: 100×). Double-label immunofluorescence to detect Neurofilament L (**G**–**I**) and GFAP (glial fibrillary acidic protein) (**J**–**L**) showed that the neuron-specific intermediate filament Neurofilament L (Neurofilament light chain) immunoreactivity (**G**–**I**) was not detectably altered in Sulf1 (**H**) and Sulf2 (**s**) deficient mutants (630×). Immunohistochemical localization of the astrocyte-specific marker GFAP (**J**–**L**) showed a normal distribution in the cerebellum of Sulf1 (**K**) and Sulf2 (**L**) mutant mice (630×). Sections G–L were counterstained with DAPI (**M**–**O**).

Figure S3. Unaltered basal synaptic transmission in 1- and 3-month-old Sulf2 **(A, C, E, G)** and Sulf1 (**B, D, F, H**) deficient mice, but impaired LTP in 1-month-old mice lacking Sulf1 function. (**A, B**) Input-output curves for slopes of fEPSPs evoked by stimulation of Schaffer collaterals at different stimulation

© 2008 The Authors
Journal compilation © 2009 Foundation for Cellular and Molecular Medicine/Blackwell Publishing Ltd

strengths. Inset shows the ratio of fEPSP amplitude to fibre volley at 50% stimulation strength for both genotypes. No significant differences between genotypes were found (**A**: $n = 9$ for wild-type and $n = 10$ for knockout, **B**: $n = 8$ for wild-type and $n = 10$ for knockout). (**C, D**) Paired-pulse facilitation (PPF) was measured as the ratio between the slopes of fEPSPs evoked by the second and first pulses and plotted for several interpulse intervals. Field EPSPs were recorded at ~40% from the subthreshold strength to evoke fPopulation spikes. To measure the second slopes of overlapping fEPSPs evoked by paired-pulse stimulation (for interpulse intervals $<$50 ms), fEPSPs evoked by a single-pulse stimulation were subtracted from fEPSPs evoked by paired-pulse stimulation. No significant differences between genotypes were found (**C**: $n = 9$ for wild-type and $n = 10$ for knockout, **D**: $n = 8$ for wild-type and $n = 10$ for knockout). (**E–H**) Bar diagrams and cumulative plots representing levels of PTP and LTP from all experiments. (**E, G**) No difference in PTP (**D**) or LTP (**E**) was detected between wild-type and Sulf2-deficient mice at the age of 1 and 3 months. Error bars represent $\pm$S.E.M. (**F**) Mice deficient in Sulf1 showed a significantly reduced mean value of LTP but not of PTP. The *asterisk* indicates a statistically significant difference (Student's t-test, $P < 0.05$). (H) Cumulative plots representing levels of PTP (triangles) and LTP (circles) from all experiments. Each *symbol* represents a single experiment. Lower values of LTP were evident for Sulf1-deficient mutants when compared with wild-type littermates. For subfigures A, C, E, G, black denotes wild-type and gray Sulf2 deficiency, for subfigures B, D, F, H, black denotes wild-type and gray Sulf1 deficiency. *n* indicates the number of tested slices.

This material is available as part of the online article from: http://www.blackwell-synergy.com/doi/abs/10.1111/j.1582-4934.2008.00558.x
(This link will take you to the article abstract).

Please note: Wiley-Blackwell are not responsible for the content or functionality of any supporting materials supplied by the authors. Any queries (other than missing material) should be directed to the corresponding author for the article.

References

1. **Bandtlow CE**, **Zimmermann DR**. Proteoglycans in the developing brain: new conceptual insights for old proteins. *Physiol Rev.* 2000; 80: 1267–90.
2. **Bovolenta P**, **Fernaud-Espinosa I**. Nervous system proteoglycans as modulators of neurite outgrowth. *Prog Neurobiol.* 2000; 61: 113–32.
3. **Lee JS**, **Chien CB**. When sugars guide axons: insights from heparan sulphate proteoglycan mutants. *Nat Rev Genet.* 2004; 5: 923–35.
4. **Van Vactor D**, **Wall DP**, **Johnson KG**. Heparan sulfate proteoglycans and the emergence of neuronal connectivity. *Curr Opin Neurobiol.* 2006; 16: 40–51.
5. **Bernfield M**, **Gotte M**, **Park PW**, ***et al***. Functions of cell surface heparan sulfate proteoglycans. *Annu Rev Biochem.* 1999; 68: 729–77.
6. **Esko JD**, **Lindahl U**. Molecular diversity of heparan sulfate. *J Clin Invest.* 2001; 108: 169–73.
7. **Turnbull J**, **Powell A**, **Guimond S**. Heparan sulfate: decoding a dynamic multifunctional cell regulator. *Trends Cell Biol.* 2001; 11: 75–82.
8. **Inatani M**, **Irie F**, **Plump AS**, ***et al***. Mammalian brain morphogenesis and midline axon guidance require heparan sulfate. *Science.* 2003; 302: 1044–6.
9. **Grobe K**, **Esko JD**. Regulated translation of heparan sulfate N-acetylglucosamine N-deacetylase/n-sulfotransferaseisozymes by structured 5′-untranslated regions and internal ribosome entry sites. *J Biol Chem.* 2002; 277: 30699–706.
10. **Pratt T**, **Conway CD**, **Tian NM**, ***et al.*** Heparan sulphation patterns generated by specific heparan sulfotransferase enzymes direct distinct aspects of retinal axon guidance at the optic chiasm. *J Neurosci.* 2006; 26: 6911–23.
11. **Ai X**, **Do AT**, **Kusche-Gullberg M**, ***et al.*** Substrate specificity and domain functions of extracellular heparan sulfate 6-O-endosulfatases, QSulf1 and QSulf2. *J Biol Chem.* 2006; 281: 4969–76.
12. **Morimoto-Tomita M**, **Uchimura K**, **Werb Z**, ***et al.*** Cloning and characterization of two extracellular heparin-degrading endosulfatases in mice and humans. *J Biol Chem.* 2002; 277: 49175–85.
13. **Lamanna WC**, **Baldwin RJ**, **Padva M**, ***et al.*** Heparan sulfate 6-O-endosulfatases: discrete *in vivo* activities and functional cooperativity. *Biochem J.* 2006; 400: 63–73.
14. **Lamanna WC**, **Kalus I**, **Padva M**, ***et al.*** The heparanome – the enigma of encoding and decoding heparan sulfate sulfation. *J Biotechnol.* 2007; 129: 290–307.
15. **Ai X**, **Kitazawa T**, **Do AT**, ***et al.*** SULF1 and SULF2 regulate heparan sulfate-mediated GDNF signaling for esophageal innervation. *Development.* 2007; 134: 3327–38.
16. **Holst CR**, **Bou-Reslan H**, **Gore BB**, ***et al.*** Secreted sulfatases Sulf1 and Sulf2 have overlapping yet essential roles in mouse neonatal survival. *PLoS ONE.* 2007; 2: e575.
17. **Lum DH**, **Tan J**, **Rosen SD**, ***et al.*** Gene trap disruption of the mouse heparan sulfate 6-O-endosulfatase gene, Sulf2. *Mol Cell Biol.* 2007; 27: 678–88.
18. **Dhoot GK**, **Gustafsson MK**, **Ai X**, ***et al.*** Regulation of Wnt signaling and embryo patterning by an extracellular sulfatase. *Science.* 2001; 293: 1663–6.
19. **Lai J**, **Chien J**, **Staub J**, ***et al.*** Loss of HSulf-1 up-regulates heparin-binding growth factor signaling in cancer. *J Biol Chem.* 2003; 278: 23107–17.
20. **Lai JP**, **Chien J**, **Strome SE**, ***et al.*** HSulf-1 modulates HGF-mediated tumor cell invasion and signaling in head and neck squamous carcinoma. *Oncogene.* 2004; 23: 1439–47.
21. **Nawroth R**, **van Zante A**, **Cervantes S**, ***et al.*** Extracellular sulfatases, elements of the wnt signaling pathway, positively regulate growth and tumorigenicity of human pancreatic cancer cells. *PLoS ONE.* 2007; 2: e392.
22. **Viviano BL**, **Paine-Saunders S**, **Gasiunas N**, ***et al.*** Domain-specific modification of heparan sulfate by Qsulf1 modulates the binding of the bone morphogenetic protein antagonist Noggin. *J Biol Chem.* 2004; 279: 5604–11.
23. **Wang S**, **Ai X**, **Freeman SD**, ***et al.*** QSulf1, a heparan sulfate 6-O-endosulfatase, inhibits fibroblast growth factor signaling in mesoderm induction and angiogenesis. *Proc Natl Acad Sci USA.* 2004; 101: 4833–8.
24. **Lamanna WC**, **Frese MA**, **Balleininger M**, ***et al.*** Sulf loss influences N-, 2O-, and

© 2008 The Authors
Journal compilation © 2009 Foundation for Cellular and Molecular Medicine/Blackwell Publishing Ltd

6O-sulfation of multiple heparan sulfate proteoglycans and modulates FGF signaling. *J Biol Chem.* 2008; 283: 27724–35.

25. **Kalus I**, **Schnegelsberg B**, **Seidah NG**, ***et al.*** The proprotein convertase PC5A and a metalloprotease are involved in the proteolytic processing of the neural adhesion molecule L1. *J Biol Chem.* 2003; 278: 10381–8.
26. **Ahlemeyer B**, **Baumgart-Vogt E**. Optimized protocols for the simultaneous preparation of primary neuronal cultures of the neocortex, hippocampus and cerebellum from individual newborn (P0.5) C57Bl/6J mice. *J Neurosci Methods.* 2005; 149: 110–20.
27. **Schmitz D**, **Mellor J**, **Breustedt J**, ***et al.*** Presynaptic kainate receptors impart an associative property to hippocampal mossy fiber long-term potentiation. *Nat Neurosci.* 2003; 6: 1058–63.
28. **Schrander-Stumpel C**, **Fryns JP**. Congenital hydrocephalus: nosology and guidelines for clinical approach and genetic counselling. *Eur J Pediatr.* 1998; 157: 355–62.
29. **Nagamine S**, **Koike S**, **Keino-Masu K**, ***et al.*** Expression of a heparan sulfate remodeling enzyme, heparan sulfate 6-O-endosulfatase sulfatase FP2, in the rat nervous system. *Brain Res Dev Brain Res.* 2005; 159: 135–43.
30. **Ohto T**, **Uchida H**, **Yamazaki H**, ***et al.*** Identification of a novel nonlysosomal sulphatase expressed in the floor plate, choroid plexus and cartilage. *Genes Cells.* 2002; 7: 173–85.
31. **Kamiguchi H**, **Hlavin ML**, **Lemmon V**. Role of L1 in neural development: what the knockouts tell us. *Mol Cell Neurosci.* 1998; 12: 48–55.
32. **Copp AJ**. Neurulation in the cranial region–normal and abnormal. *J Anat.* 2005; 207: 623–35.
33. **Dityatev A**, **Dityateva G**, **Sytnyk V**, ***et al.*** Polysialylated neural cell adhesion molecule promotes remodeling and formation of hippocampal synapses. *J Neurosci.* 2004; 24: 9372–82.
34. **Rauvala H**, **Peng HB**. HB-GAM (heparin-binding growth-associated molecule) and heparin-type glycans in the development and plasticity of neuron-target contacts. *Prog Neurobiol.* 1997; 52: 127–44.
35. **Manabe T**, **Wyllie DJ**, **Perkel DJ**, ***et al.*** Modulation of synaptic transmission and long-term potentiation: effects on paired pulse facilitation and EPSC variance in the CA1 region of the hippocampus. *J Neurophysiol.* 1993; 70: 1451–9.
36. **Grove EA**. Neuroscience. Organizing the source of memory. *Science.* 2008; 319: 288–9.
37. **Danesin C**, **Agius E**, **Escalas N**, ***et al.*** Ventral neural progenitors switch toward an oligodendroglial fate in response to increased Sonic hedgehog (Shh) activity: involvement of Sulfatase 1 in modulating Shh signaling in the ventral spinal cord. *J Neurosci.* 2006; 26: 5037–48.
38. **Zhao W**, **Sala-Newby GB**, **Dhoot GK**. Sulf1 expression pattern and its role in cartilage and joint development. *Dev Dyn.* 2006; 235: 3327–35.
39. **Sala-Newby GB**, **George SJ**, **Bond M**, ***et al.*** Regulation of vascular smooth muscle cell proliferation, migration and death by heparan sulfate 6-O-endosulfatase1. *FEBS Lett.* 2005; 579: 6493–8.
40. **Bullock SL**, **Fletcher JM**, **Beddington RS**, ***et al.*** Renal agenesis in mice homozygous for a gene trap mutation in the gene encoding heparan sulfate 2-sulfotransferase. *Genes Dev.* 1998; 12: 1894–906.
41. **Ringvall M**, **Ledin J**, **Holmborn K**, ***et al.*** Defective heparan sulfate biosynthesis and neonatal lethality in mice lacking N-deacetylase/N-sulfotransferase-1. *J Biol Chem.* 2000; 275: 25926–30.
42. **Shworak NW**, **HajMohammadi S**, **de Agostini AI**, ***et al.*** Mice deficient in heparan sulfate 3-O-sulfotransferase-1: normal hemostasis with unexpected perinatal phenotypes. *Glycoconj J.* 2002; 19: 355–61.
43. **Uchimura K**, **Morimoto-Tomita M**, **Bistrup A**, ***et al.*** HSulf-2, an extracellular endoglucosamine-6-sulfatase, selectively mobilizes heparin-bound growth factors and chemokines: effects on VEGF, FGF-1, and SDF-1. *BMC Biochem.* 2006; 7: 2.
44. **Pellegrini L**, **Burke DF**, **von Delft F**, ***et al.*** Crystal structure of fibroblast growth factor receptor ectodomain bound to ligand and heparin. *Nature.* 2000; 407: 1029–34.
45. **Schlessinger J**, **Plotnikov AN**, **Ibrahimi OA**, ***et al.*** Crystal structure of a ternary FGF-FGFR-heparin complex reveals a dual role for heparin in FGFR binding and dimerization. *Mol Cell.* 2000; 6: 743–50.
46. **Deng C**, **Bedford M**, **Li C**, ***et al.*** Fibroblast growth factor receptor-1 (FGFR-1) is essential for normal neural tube and limb development. *Dev Biol.* 1997; 185: 42–54.
47. **Dono R**, **Texido G**, **Dussel R**, ***et al.*** Impaired cerebral cortex development and blood pressure regulation in FGF-2-deficient mice. *EMBO J.* 1998; 17: 4213–25.
48. **Arikawa-Hirasawa E**, **Watanabe H**, **Takami H**, ***et al.*** Perlecan is essential for cartilage and cephalic development. *Nat Genet.* 1999; 23: 354–8.
49. **Giros A**, **Morante J**, **Gil-Sanz C**, ***et al.*** Perlecan controls neurogenesis in the developing telencephalon. *BMC Dev Biol.* 2007; 7: 29.
50. **Kinnunen T**, **Raulo E**, **Nolo R**, ***et al.*** Neurite outgrowth in brain neurons induced by heparin-binding growth-associated molecule (HB-GAM) depends on the specific interaction of HB-GAM with heparan sulfate at the cell surface. *J Biol Chem.* 1996; 271: 2243–8.
51. **Riopelle RJ**, **Dow KE**. Functional interactions of neuronal heparan sulphate proteoglycans with laminin. *Brain Res.* 1990; 525: 92–100.
52. **Kato K**, **Utani A**, **Suzuki N**, ***et al.*** Identification of neurite outgrowth promoting sites on the laminin alpha 3 chain G domain. *Biochemistry.* 2002; 41: 10747–53.
53. **Kim MJ**, **Cotman SL**, **Halfter W**, ***et al.*** The heparan sulfate proteoglycan agrin modulates neurite outgrowth mediated by FGF-2. *J Neurobiol.* 2003; 55: 261–77.
54. **Kurosawa N**, **Chen GY**, **Kadomatsu K**, ***et al.*** Glypican-2 binds to midkine: the role of glypican-2 in neuronal cell adhesion and neurite outgrowth. *Glycoconj J.* 2001; 18: 499–507.
55. **Dityatev A**, **Schachner M**. The extracellular matrix and synapses. *Cell Tissue Res.* 2006; 326: 647–54.
56. **Lauri SE**, **Kaukinen S**, **Kinnunen T**, ***et al.*** Regulatory role and molecular interactions of a cell-surface heparan sulfate proteoglycan (N-syndecan) in hippocampal long-term potentiation. *J Neurosci.* 1999; 19: 1226–35.
57. **Goddyn H**, **Leo S**, **Meert T**, ***et al.*** Differences in behavioural test battery performance between mice with hippocampal and cerebellar lesions. *Behav Brain Res.* 2006; 173: 138–47.
58. **Kaksonen M**, **Pavlov I**, **Voikar V**, ***et al.*** Syndecan-3-deficient mice exhibit enhanced LTP and impaired hippocampus-dependent memory. *Mol Cell Neurosci.* 2002; 21: 158–72.
59. **Pavlov I**, **Voikar V**, **Kaksonen M**, ***et al.*** Role of heparin-binding growth-associated molecule (HB-GAM) in hippocampal LTP and spatial learning revealed by studies on overexpressing and knockout mice. *Mol Cell Neurosci.* 2002; 20: 330–42.
60. **Cornelison DD**, **Wilcox-Adelman SA**, **Goetinck PF**, ***et al.*** Essential and separable roles for Syndecan-3 and Syndecan-4 in skeletal muscle development and regeneration. *Genes Dev.* 2004; 18: 2231–6.

© 2008 The Authors
Journal compilation © 2009 Foundation for Cellular and Molecular Medicine/Blackwell Publishing Ltd